Tau Identification in the Second Level Trigger

Beatriz Gonzalez Pineiro
Michigan State University

Abstract

The studies to optimize an algorithm for tau identification in the LVL2 trigger are presented. The trigger rate obtained by combining calorimeter and tracking information is estimated.

Introduction

Tau identification relies on the selection of narrow, isolated jets associated with few tracks in the tracking system. The shower shape and isolation are calculated for both the e.m. and hadronic calorimeters separately. The fraction of energy deposited by a tau-jet in the e.m. calorimeter is on average 60%; the hadronic shower is narrower in the e.m. calorimeter than in the hadronic calorimeter. For these reasons the e.m. information is more selective in the tau jet separation than the information from the hadronic calorimeter.

The following sections describe the two steps of the calorimeter tau algorithm: verification of the LVL1 decision, and tau identification using parameters that describe the shower shape and the isolation of the narrow jet. Simple quantities which can be calculated quickly are used. The cluster information from the calorimeter is finally combined with track information to identify the tau candidate. After optimization of the algorithm parameters, the expected trigger rate for jets is estimated. The results of the study are presented in the Trigger Performance Status Report [0-1].

Data Sets

The signal selection is tuned using events of the type $A^0 \rightarrow \tau\tau$; the rejection of background from jets is optimised using QCD jet samples. The signal sample consists of 2500 fully simulated events of τ-jets from two samples of $A^0 \rightarrow \tau\tau$ events: associated bbA^0 production, and single A^0 production (m_A = 150, 300 and 450 GeV). One of the τ's is forced to decay leptonically via $\tau \rightarrow \mu\nu_\mu$. More details on this event sample can be found in [0-2].

For background evaluation fully simulated di-jet candidates from the standard jet production were used [0-3]. These events were pre-selected at particle level by requiring at least two regions of size $d\eta \times d\phi = 1.0 \times 1.0$ with transverse energy exceeding 40 GeV. The sample was biased by requiring the second jet to be more energetic than the first found and allows only relative comparison of different algorithms, but can not be used for extracting trigger rates. The trigger rates were calculated using the LVL1 jet production, where the event selection is unbiased for tau studies.

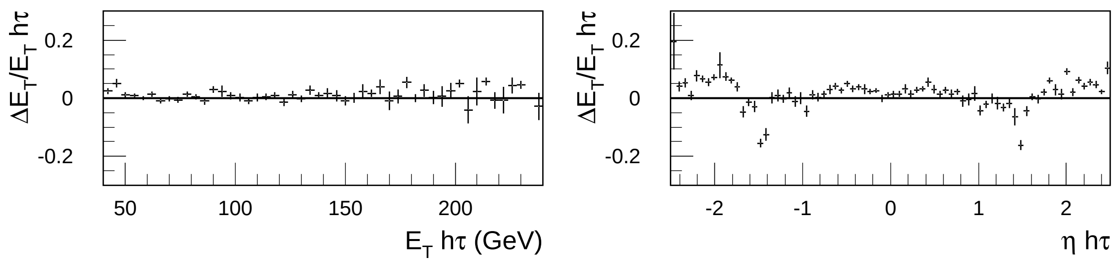

Figure 0-1 E_T and η dependence of the relative difference between the energies of the hadronic decay part of the tau at particle level, and the reconstructed jet associated to the tau: $(E_{Tj\tau}\text{-}E_{Th\tau})/E_{Th\tau}$, after tau labelling.

Labelling of Tau-jets

To determine the efficiency for selecting taus, it is necessary to identify the jet associated to the generated lepton. For this, the hadronic decay part of the tau ('hadronic tau' for short) is used to compute at particle level (KINE) the energy weighted position ($\eta_{h\tau}$, $\phi_{h\tau}$). This is compared with the energy weighted position of each reconstructed jet ($\eta_{j\tau}$, $\phi_{j\tau}$) tagged as a τ by LVL1 [0-1]. Only the cells in the LVL1 window ($\Delta\eta \times \Delta\phi = 0.4 \times 0.4$) are used in the calculation. A LVL1 RoI is labelled as 'tau-jet' if $|\eta_{j\tau}-\eta_{h\tau}|<0.3$ and $|\phi_{j\tau}-\phi_{h\tau}|<0.3$. The widths of the corresponding distributions are $\sigma_{\Delta\eta}=0.026$ and $\sigma_{\Delta\phi}=0.010$, indicating that the LVL1 RoI coordinates are good approximations of the hadronic tau coordinates. The tau labelling efficiency is 96.3%, slightly lower than the efficiency of 98% achieved with full event reconstruction [0-2].

A cross check of the quality of the labelling can be obtained by comparing the transverse energies of the tau-jet and the corresponding hadronic tau. In order to calculate the energy of the reconstructed tau, the jet calibration factors (see Table 0-1) are applied to the cells within the LVL1 RoI window. The factors are averaged over the values given in [0-4]. The scintillator in the barrel/end-cap overlap region is not used; future versions of the algorithm will use the scintillator and apply an improved calibration.

Table 0-1 Jet Calibration factors applied to cells selected within the LVL1 RoIs [0-4].

Subdetector	Calibration
Pre-Shower	1.10
Accordion	1.10
EM End Cap	1.10
Tile Calorimeter	1.05
Had End Cap	1.25

Figure 0-1 shows the relative difference between the considered energies $(E_{Tj\tau}\text{-}E_{Th\tau})/E_{Th\tau}$ as a function of E_T and η of the hadronic tau.The behaviour does not depend on the energy of the tau. The jet energy is slightly overestimated; however the differences are smaller than 5% in all range of energies.

There is a more important dependence on eta. The loss of energy in the crack region is related with the energy left in the scintillator, not yet included in the reconstruction. The jet energy is overestimated by 3% in the barrel and by 6% in the endcap, on average. This effect is due to the different electromagnetic and hadronic composition of a tau jet in comparison with a QCD jet, which is assumed in the jet calibration. No dependence on ϕ has been observed.

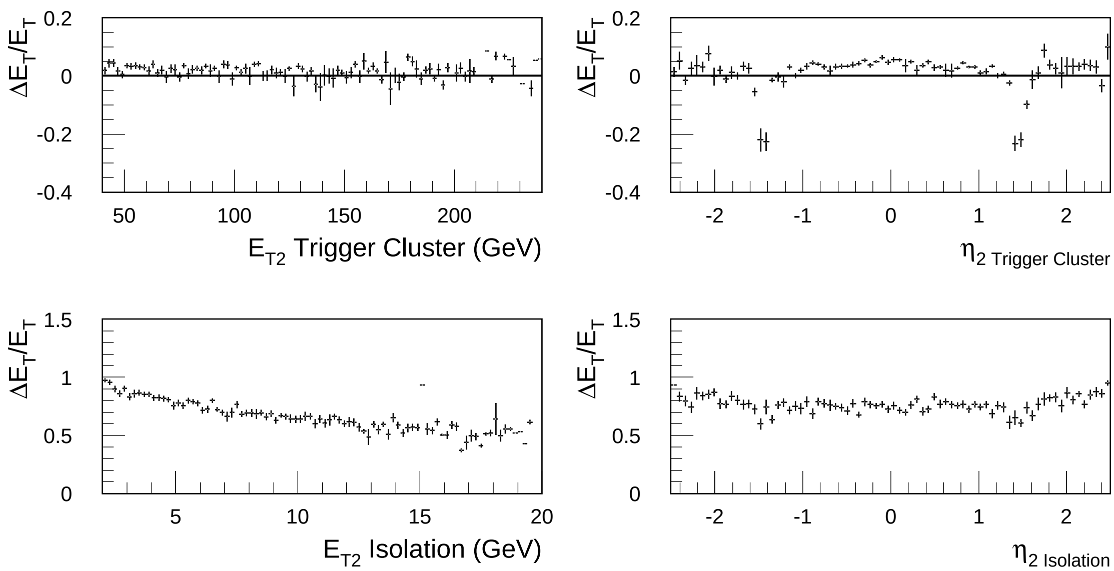

Figure 0-2 Comparison of LVL1 RoI quantities (E_{T1}, η_1) and quantities calculated by a LVL1-like algorithm applied at LVL2 (E_{T2},η_2): $\Delta E_T/E_{T2}$ where $\Delta E_T = E_{T2} - E_{T1}$, for trigger cluster (top) and isolation window (bottom) versus E_{T2} and η_2.

Verification of LVL1

The first step of the LVL2 algorithm is the confirmation of the LVL1 decision. The LVL1 algorithm is described in reference [0-1], chapter 6. The same algorithm as at LVL1 is executed, except that the fine-grained cell information is used and no threshold is applied to trigger towers. At LVL1 this threshold is 1 GeV. The windows for core and isolation measurements are the same as those used by the LVL1 algorithm: the trigger cluster, defined as the most energetic $\Delta\eta \times \Delta\phi = 0.1 \times 0.2$ cluster in the 0.2×0.2 inner part of the RoI, and the isolation window, composed by the outer trigger towers in the LVL1 window 0.4×0.4 minus core of 0.2×0.2.

Figure 0-2 shows the E_T and η dependence of the relative difference $(E_{T2}-E_{T1})/E_{T2}$ between the RoI energy reconstructed at LVL1 and LVL2 for the trigger cluster and for the isolation window.The threshold applied at LVL1 affects both the cluster and the isolation E_T. The cluster energies reconstructed at LVL2 are slightly higher (5%). The effect is more significant for the isolation energies, for which twelve trigger towers with low energy are summed. The loss of energy in the crack region around η=1.5 is due to the fact that the scintillator energy is not used at LVL2. At LVL1 the calibration compensates partially for the loss of energy in the transition region. Despite the loss, the efficiency for labelling τ's is only 0.3% lower for LVL2 than for LVL1.

LVL2 Tau Algorithm

The LVL2 tau algorithm is applied to the τ RoIs selected by the LVL1. Loose LVL1 cuts are chosen for the study presented here: a trigger cluster E_T greater than 30 GeV is required, and e.m. and hadronic isolation thresholds are set to 10 GeV.

The core window is now centred at the energy weighted position ($\eta_{j\tau}$,$\phi_{j\tau}$). The performance of the algorithm is studied for several choices of the size of the electromagnetic core: $\Delta\eta \times \Delta\phi = 0.10 \times 0.10$, 0.15×0.15, 0.20×0.20 and 0.25×0.25. Since the hadronic granularity does not change, the hadronic core size is chosen to be the same as for LVL1, 0.20 × 0.20. Isolation windows are defined separately for the e.m. or hadronic parts as the complement of the respective core and the 0.40 × 0.40 RoI region. Isolation thresholds are defined for e.m. and hadronic contributions separately.

The performance as a function of the core size is studied for three values of the integrated efficiency for jets: 20%, 30% and 40%. Each of these values is obtained by applying a different threshold to the core energy. Using this threshold it is possible to determine the efficiency for the tau sample. Efficiencies are normalised relative to the events accepted by LVL1. Obtained thresholds and tau efficiencies are listed in Table 0-2. For the first four columns the threshold is applied to the sum of the transverse energies in the

Table 0-2 Comparison of several tau core algorithms for LVL2. Thresholds, in GeV, and associated tau efficiencies are given for three sets of fixed jet efficiencies. For combined algorithms the hadronic size is always $\Delta\eta \times \Delta\phi$ = 0.20 × 0.20.

	EM +Had								**pure EM**			
	0.10 × 0.10		**0.15 × 0.15**		**0.20 × 0.20**		**0.25 × 0.25**		**0.10 × 0.10**		**0.15 × 0.15**	
Jet Eff	**Thr**	ε_τ	**Thr**	ε_τ	**Thr**	ε_τ	**Thr**	ε_τ	**Thr**	ε_τ	**Thr**	ε_τ
40%	45.0	82.0%	50.0	79.0%	53.0	77.0%	55.0	76.0%	31.5	72.0%	38.0	68.0%
30%	49.0	76.0%	55.0	73.0%	58.0	71.0%	60.0	69.5%	35.5	66.0%	41.5	62.0%
20%	57.0	67.0%	63.0	64.0%	66.0	72.0%	68.0	61.5%	40.0	59.0%	47.0	55.5%

e.m. and hadronic core, the last two columns show results for the case when only the e.m. core is used. In order to keep the same jet efficiency with increasing core size, the threshold has to increase. The efficiency as a function of the hadronic part of the tau energy is shown in Figure 0-3. For the small-sized core combined with the hadronic core an efficiency exceeding 80% can be reached for E_T > 75, 65 and 60 GeV, and jet efficiencies of 20%, 30% and 40%, respectively. The last two columns in the table correspond to the use of the pure e.m. core for small core sizes. In this case no sharp threshold can be achieved.

To optimize the isolation criteria only the core types with best performance are retained: 0.10 × 0.10 or 0.15 × 0.15 electromagnetic core plus 0.2 × 0.2 hadronic core. The dependence of the efficiency on the em isolation E_T is shown in Figure 0-4. The case of the 0.15 × 0.15 core exhibits a sharper rise and longer plateau. For an isolation threshold of 10 GeV the jet rate is reduced by a factor of two, while keeping the tau efficiency at 73%. Hadronic isolation has less rejection power. This is also illustrated in Figure 0-5, where tau efficiency is shown as a function of the jet efficiency. The parameter varied is the e.m. or hadronic isolation threshold. To optimize signal selection and background rejection, a 0.15 × 0.15 core algorithm with e.m. isolation is preferred. Tau efficiency versus tau hadronic energy is shown in Figure 0-5, after applying core and e.m. or hadronic isolation thresholds. Points are shown for the three different threshold values applied to the core, see Table 0-2. The isolation cut affects only the high energy taus.

Instead of using the absolute energy in the isolation window, relative energy fractions can be computed. This avoids possible losses of high energy taus. Two quantities were considered: the fraction of total energy in the isolation windows and the fraction of e.m. energy in the core. Both quantities have a similar rejection power for the same signal efficiency, see Figure 0-6. The latter, used in previous studies [0-2], is retained. The distribution is shown in Figure 0-6. The value indicated by the arrow, E_T^{core} (em) /E $_T$ (em) > 0.85, gives a jet rejection of about a factor two, while keeping the tau efficiency at 70%.

Finally the energy weighted radius was considered. It is calculated using all cells in the 0.4 × 0.4 window. Distributions of the energy weighted radius are shown in Figure 0-7. While tau/jet separation is difficult using hadronic information only, the e.m. radius provides better discrimination, particularly when only

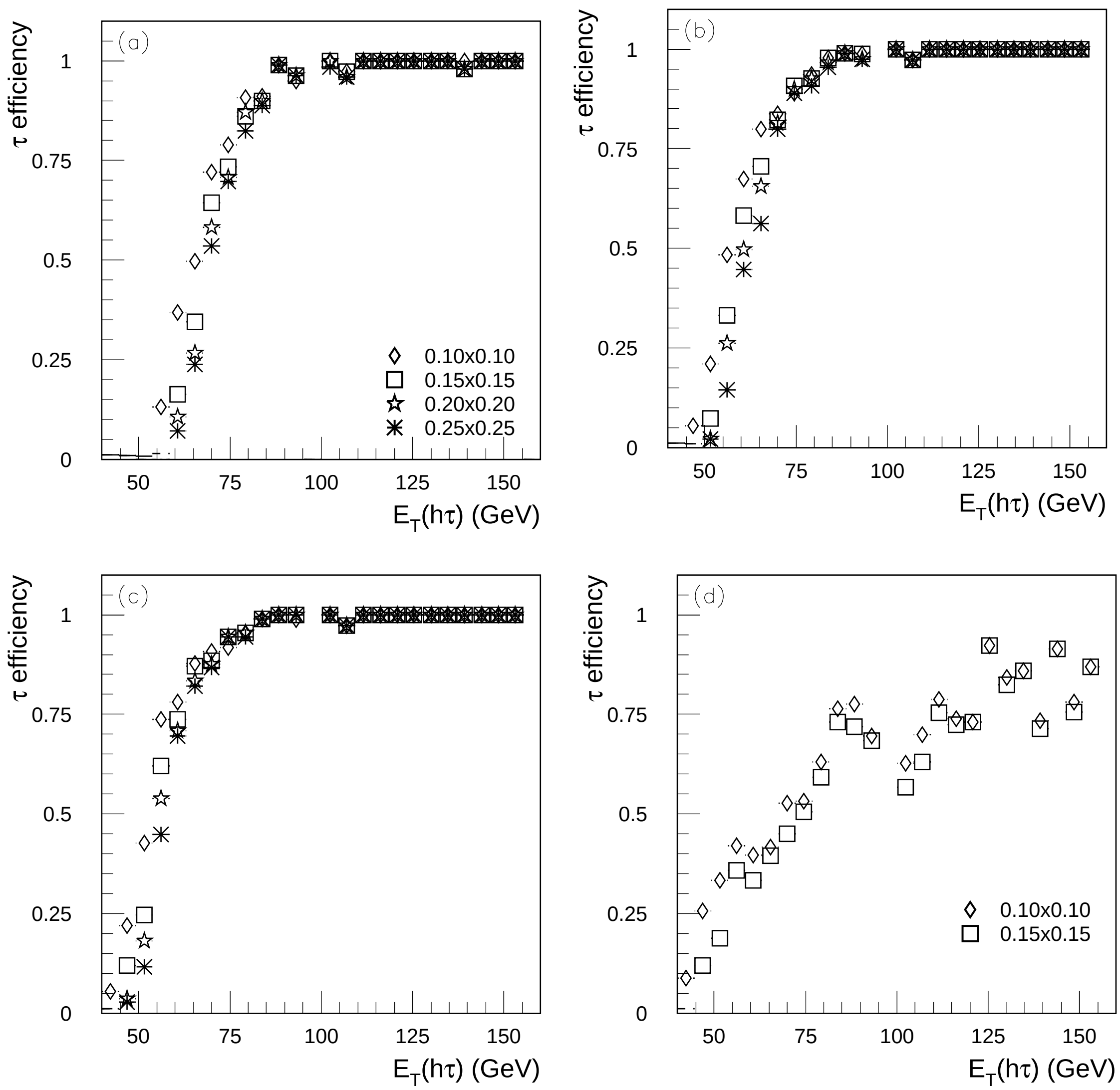

Figure 0-3 Tau efficiency versus hadronic tau energy for several core sizes and for fixed values of jet efficiency: (a) 20%, (b) 30%, (c) 40%, (d) 40% with electromagnetic core only. See also Table 0-2.

calorimeter sampling 2 is used. However, as the energy weighted radius and the energy fractions are strongly correlated, the use of fractions, which are faster to compute, is preferred.

Resulting tau and jet efficiencies versus measured energy in the 0.4×0.4 window are shown in Figure 0-7. These quantities refer to the efficiency for taus or jets already selected by LVL1 as τ candidates. The selected cuts were sequentially applied: first, the minimum energy in the core was set to 50 GeV in order to have 40% jet efficiency. Second, the fraction of electromagnetic energy in the core was required to be in excess of 85%. The second cut reduces the jet efficiency by a factor of two, while keeping efficiencies in excess of 75% for taus. Tau efficiencies exceed 90% for transverse energies higher than 60 GeV.

Tau identification with a combined algorithm

Additional rejection of background jets can be achieved by using the information from tracks associated to the τ RoI. The results presented here were obtained considering the generated charged tracks (KINE).

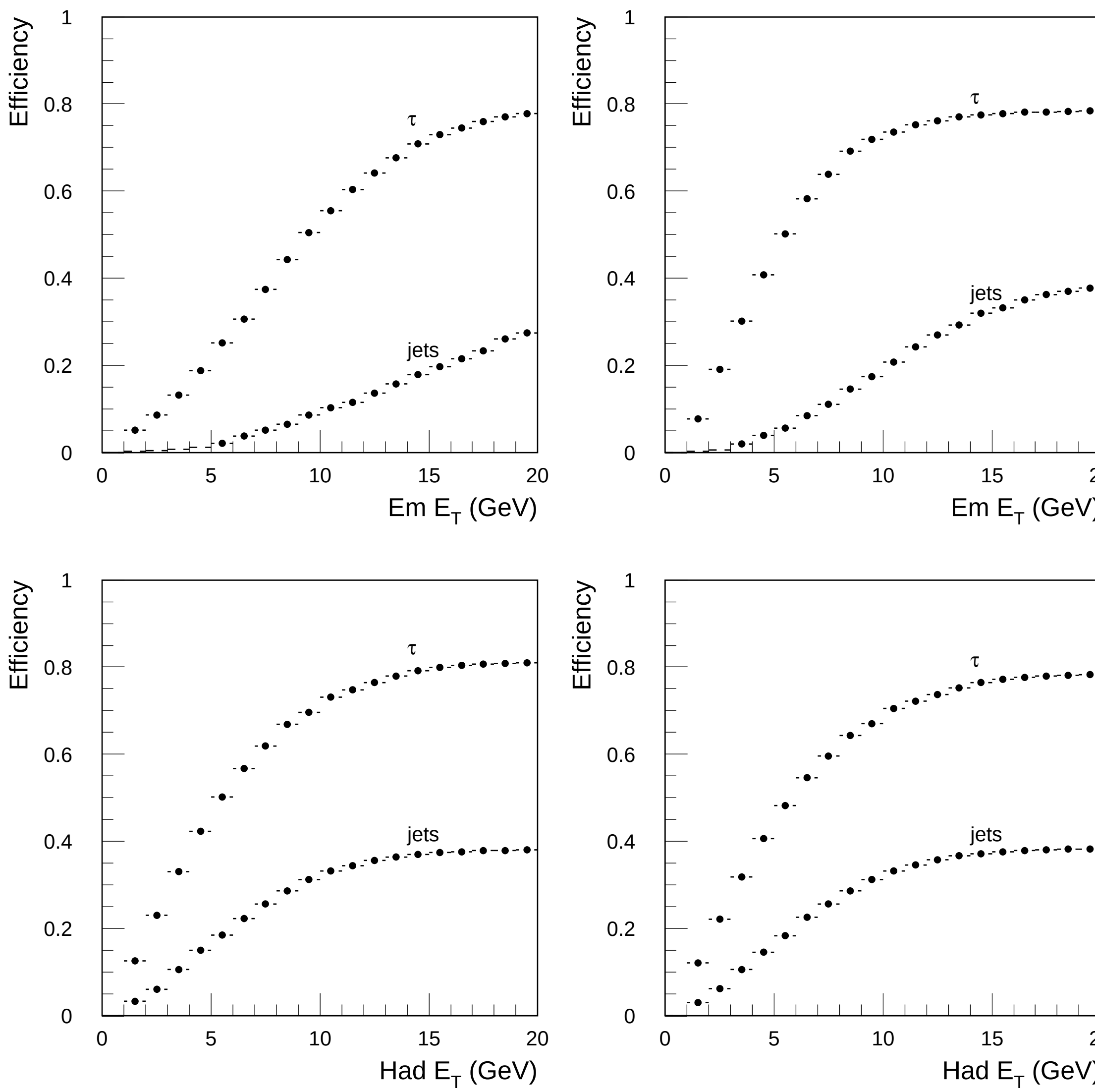

Figure 0-4 Tau and jet efficiencies versus maximum electromagnetic (up) or hadronic (down) energy allowed in isolation windows for two core sizes: 0.10×0.10 (left) and 0.15×0.15 (right). Core thresholds have been selected to have 40% jet efficiency (see Table 0-2).

Some degradation in performance is expected in a more realistic situation, where photon conversions are present and the efficiency of the track finding at the LVL2 is taken into account.

Tracks are selected within a window of $\Delta\eta \times \Delta\phi = 0.4 \times 0.4$ centred at the tau cluster. Only tracks above a p_T threshold (2 GeV or 5 GeV) are used and track efficiencies of 90% or 100% are assumed. We require either exactly one track, or one to three tracks within the window. The resulting efficiencies for taus and jets are summarized in Table 0-3. The results are presented for RoIs selected after applying the LVL1 or LVL2 calorimeter algorithms respectively.

The requirement on the number of tracks results in similar jet efficiencies for LVL1 and LVL2 RoIs, indicating that correlations between calorimeter and tracking selections are small. Assuming 100% track efficiency, and requiring $p_T > 2$ GeV and $1 \le N_{trk} \le 3$, the jet rate is reduced by approximately a factor of two, while keeping the tau efficiency close to 85%. The reduction of jets can reach about a factor of ten

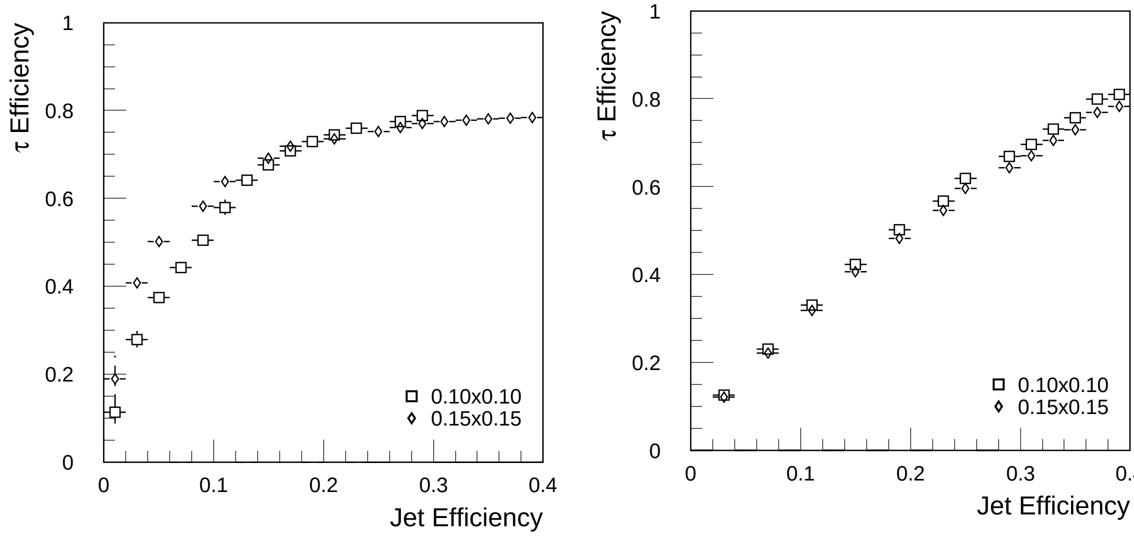

Figure 0-5 Tau versus jet efficiency for core sizes with best performance. The points correspond to different electromagnetic (left) or hadronic (right) isolation thresholds, varying from 0 to 20 GeV.

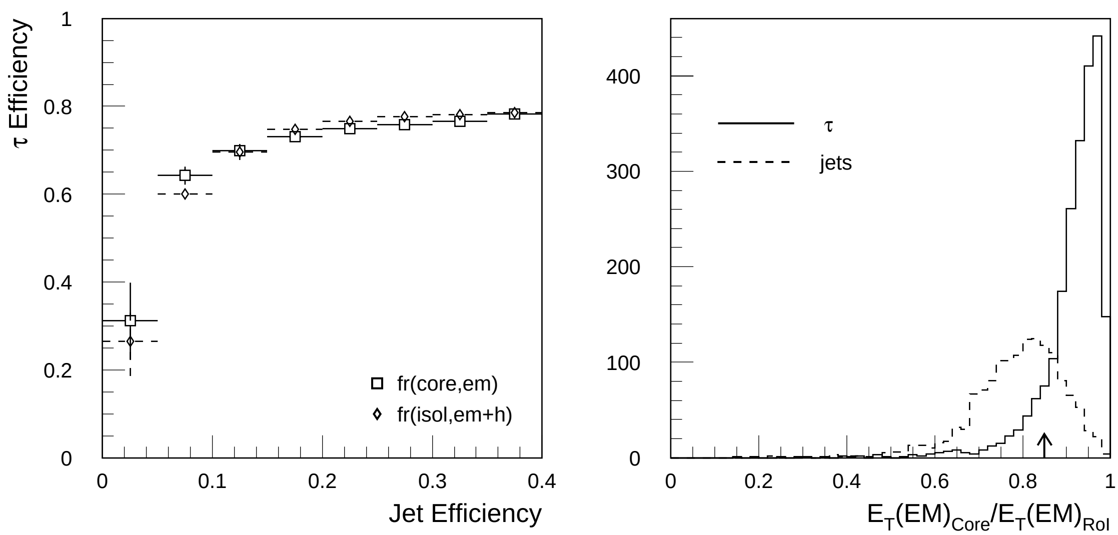

Figure 0-6 Left: Tau versus jet efficiency obtained varying the cuts on the fraction of total energy in the isolation window E_T^{isol} (em+h)/E_T (em+h) and the fraction of electromagnetic energy in the core E_T^{core} (em) /E_T (em). Right: Fraction of electromagnetic energy in the core. Core sizes are 0.15×0.15 (electromagnetic) and 0.2×0.2 (hadronic); isolation windows are their complement in a 0.40×0.40 window.

when exactly one charged track is required, but in this case the tau efficiency is reduced to less than 50%. In a more realistic simulation, where tracks due to photon conversions are present, both efficiencies could be lower.

Inefficiency in track finding reduces the jet rejection power as well as the tau efficiency. However the effect is small for realistic values of the track efficiency (90%): about 7% increase in jet rate and 3% decrease in efficiency for taus. Finally, if a higher p_T cut is chosen, $p_T > 5$ GeV, then the rejection power for

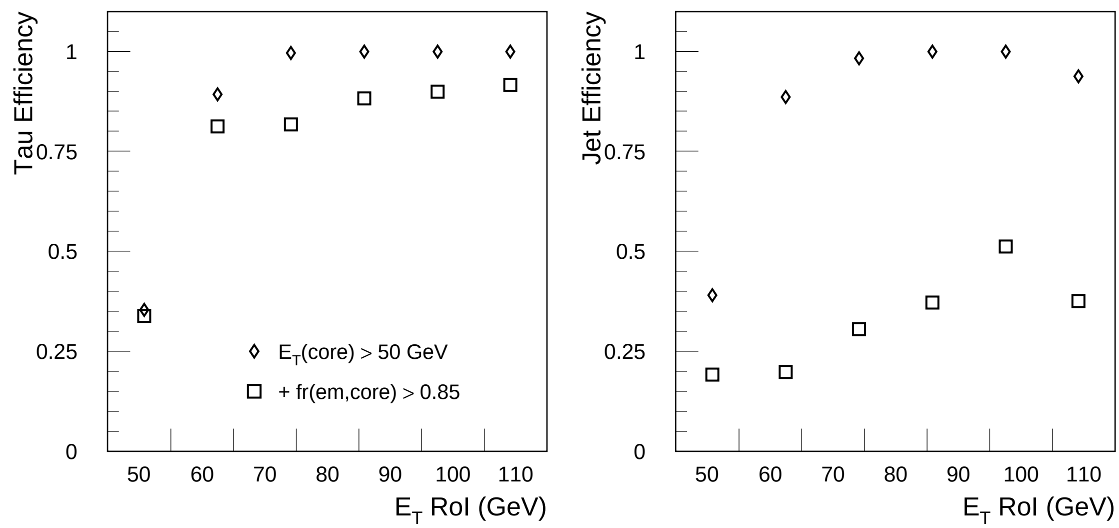

Figure 0-7 Tau (left) and jet (right) efficiencies versus measured Et in the 0.4x0.4 window for cuts applied sequentially: 1) core energy bigger than 50 GeV, 2) fraction of electromagnetic energy in the core greater than 85%.

jets is significantly diminished, with little effect on the tau efficiency. Thus, the capability of the ATLAS tracking system to measure low-p_T tracks at LVL2 will be important for tau/jet separation.

Table 0-3 Tau and jet efficiencies after a cut on the number of generated charged tracks. The results are shown when applied to LVL1 tau RoIs, and after the LVL2 tau selection in the calorimeter.

		100% = LVL1 Tau Calo RoIs				100% = LVL2 Tau Calo RoIs			
		N_{trk} = 1		$1 \le N_{trk} \le 3$		N_{trk} = 1		$1 \le N_{trk} \le 3$	
Track Eff	P_T Track	Tau eff. (%)	Jet eff. (%)	Tau eff. (%)	Jet eff. (%)	Tau eff. (%)	Jet eff. (%)	Tau eff. (%)	Jet eff. (%)
100 %	> 2 GeV	47.5	5.9	89.5	33.7	48.3	6.1	85.0	45.6
90 %	> 2 GeV	45.2	8.0	82.5	41.9	45.8	11.4	81.7	52.3
100 %	> 5 GeV	48.8	21.4	88.1	69.2	49.1	23.7	87.3	65.8
90 %	> 5 GeV	47.4	23.4	85.1	72.0	47.6	25.9	84.6	68.0

Trigger Performance

Tau/jet separation at LVL2 is based on calorimeter and tracking information. Summarizing the discussion in the previous paragraphs, we recommend the following selections. The calorimeter selection, wich is done in two steps: The e.m. plus hadronic transverse energy contained in a small core is required to be above threshold, e.g.

- E_T^{Core}(em+h) > 50 GeV.

The fraction of electromagnetic energy in the core is required to be greater than 85%,

- fr(core) = $E_T^{Core}(em)/E_T^{RoI}(em) > 0.85$.

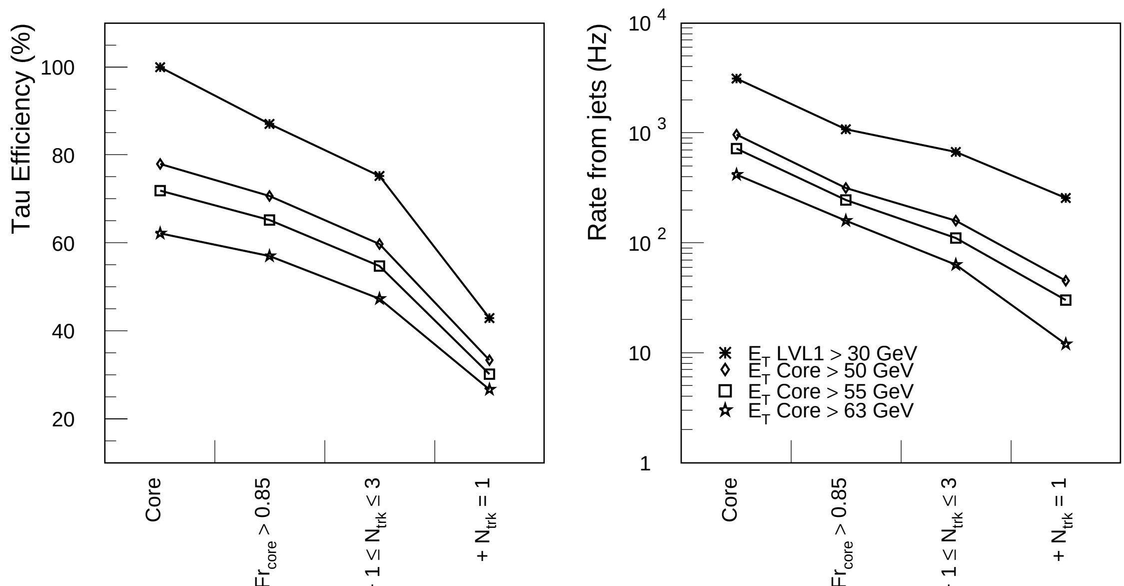

Figure 0-8 Evolution of the tau efficiency and the rate from jets (luminosity 10^{33} cm^{-2}s^{-1}), when the LVL2 tau selection criteria are applied sequentially. The different symbols correspond to different initial cuts on E_T^{Core}(em+h). The tau efficiencies are quoted with respect to LVL1. The selections are explained in the text.

Figure 0-8 shows the evolution of the tau efficiencies and the rates from jets, when these selections are applied. The E_T cut reduces the LVL1 tau trigger rates by a factor of three, and the requirement on core energy gives an additional reduction of more than a factor three, while keeping the tau efficiency close to 70%.

Additional rejection is obtained by restricting the number N_{trk} of charged tracks associated to the tau RoI, e.g. for a threshold of $p_T > 2$ GeV

- $1 \le N_{trk} \le 3$.

The resulting trigger rate is 160 Hz, and the tau efficiency is close to 60%. Further jet rejection could be obtained by requiring exactly one track; in this case the tau efficiency is reduced to ~30%. Other values for the selection criteria and the corresponding rates and efficiencies are listed in Table 0-4. This study was done using generated tracks (KINE). For a more realistic situation, converted photons and inefficiency of tracking must be considered.

Table 0-4 Rates from jets and tau efficiencies for LVL2 tau selections applied sequentially. The columns correspond to different cuts on the LVL2 core E_T. For the first column only the LVL1 cut (E_T > 30 GeV) is applied, for the remaining columns increasing cuts in core E_T are applied. The selections are explained in the text.

	LVL1 Eff_j=100%		**E_T>50 GeV Eff_j=40%**		**E_T>55 GeV Eff_j=30%**		**E_T>63 GeV Eff_j=20%**	
Selection	**Rate(Hz)**	**Eff_τ (%)**	**Rate(Hz)**	**Eff_τ (%)**	**Rate(Hz)**	**Eff_τ (%)**	**Rate(Hz)**	**Eff_τ (%)**
E_T(Core)	3105	100.0	966	78.0	719	71.8	418	62.2
+ fr^{Core} (em) >0.85	1086	87.0	316	70.6	245	65.2	158	57.0
+ $1 \le N_{trk} \le 3$	668	75.2	158	59.7	110	54.7	63	47.3
+ $N_{trk} = 1$	254	42.9	45	33.3	30	30.2	12	26.7

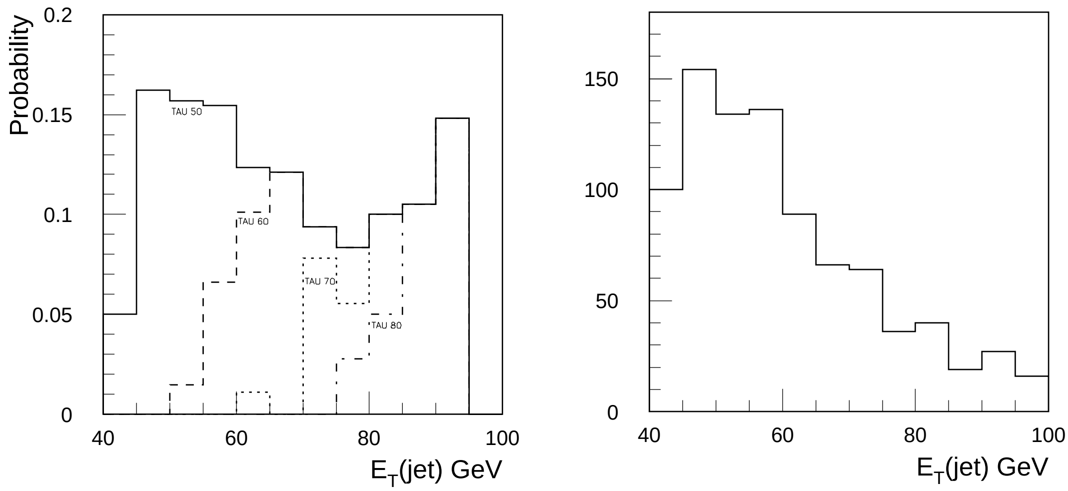

Figure 0-9 Left: Probability for a jet of energy E_T(jet) to fake a tau of energy above 50, 60, 70 or 80 GeV. Right: Distribution of the energy of the jet in the window $\Delta\eta \times \Delta\phi = 0.8 \times 0.8$.

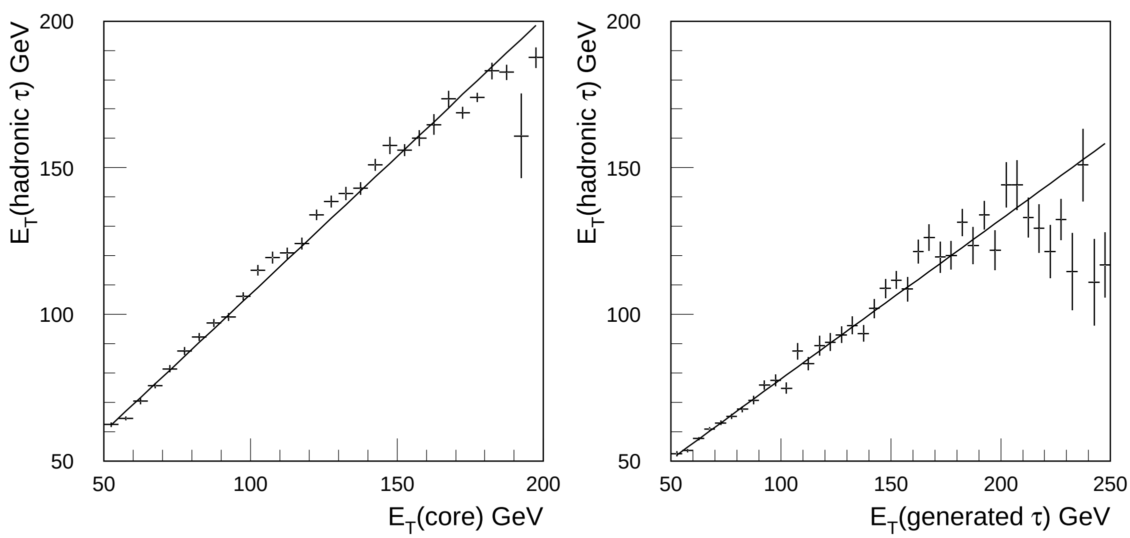

Figure 0-10 Left: Average energy of the hadronic decay part of the tau versus 1) the energy reconstructed in the core, which is used by the trigger (left). 2) The total energy of the tau (right).

The probability for a jet of a certain energy to fake a tau of energy above a minimum value is lower than 16% over the considered range, as illustrated in Figure 0-9. The probabilities should be taken as indicative, because the following approximations were made. The jet energy (see distribution in Figure 0-9, right) is defined as the energy contained in a region of size $\Delta\eta \times \Delta\phi = 0.8 \times 0.8$ around the energy weighted position of the cluster. The energy of the tau is defined by the hadronic decay part of the lepton, calculated at particle level (KINE). Figure 0-10 relates this quantity with the energy reconstructed in the core, used by the trigger. The fitted line gives the relation E_T(hadronic tau) = $0.94E_T$(core) + 12.8 GeV. The relation between the hadronic tau energy and the total energy of the tau is also shown. In this case the line corresponds to the equation E_T(hadronic tau) = $0.55E_T$(generated tau) + 23.3 GeV. These figures give only average values, which must be kept in mind in interpretating them. The latter figure shows that the contribution of the neutrino to the total energy is not negligible. In the sample used, $A^0 \rightarrow \tau\tau$, the neutrino produced by the second tau contributes also to the missing energy. A requirement on the missing energy of the event could be used to improve the tau jet separation obtained with calorimeter and track information.

Acknowledgments

The work presented here has been realised with the active help and support of M. Abolins, J. Baines, S. Georges, S. Gonzalez, T. Hansl, B. Pope and A. Watson.

0.1 References

0-1 ATLAS Trigger Performance Report, CERN (June 1998)

0-2 D. Cavalli, S.Resconi, Tau-jet separation in ATLAS detector, ATLAS Internal Note, PHYS–NO–118 (Jan 1998).

0-3 A. Dell'Acqua et al., ATLAS Internal Note, PHYS–NO–102 (1997).

0-4 ATLAS Calorimeter Performance Technical Design Report, CERN/LHCC/96–40, ATLAS TDR 1 (January 1997).